Structural and magnetic properties of nanocrystalline $Fe_{73.5-x}Co_xSi_{13.5}B_9CuNb_3$ alloys

C. Gómez-Polo*
Dept. de Física, Universidad Pública de Navarra, Campus de Arrosadía, 31006 Pamplona, Spain

P. Marín, L. Pascual, A. Hernando, and M. Vázquez
Inst. de Magnetismo Aplicado (UCM-RENFE) and Inst. de Ciencia de Materiales (CSIC), P.O. Box 155, 28230 Las Rozas, Spain

(Received 22 January 2001; revised manuscript received 30 May 2001; published 19 December 2001)

The effects of the partial substitution of Fe by Co in an FeSiBCuNb alloy on the crystallization process and on the magnetic properties have been analyzed. The crystallization of the amorphous melt-spun alloys, gives rise to an ultrafine structure composed by a residual amorphous matrix and crystals (tens of nm in size). Saturation magnetization and Curie temperature are analyzed in the nanocrystalline state in terms of the estimated compositional dependence of both structural phases. Coercivity behavior is interpreted within the framework of the random anisotropy model, where the structure and magnetic nature of the precipitated crystalline phase plays the dominant role. While a soft magnetic behavior is ascribed to the magnetic coupling between the α-FeSiCo crystals for low Co concentrations, the precipitation of Co rich crystals in the Co base samples gives rise to a drastic magnetic hardening. The main interest of these new soft magnetic FeCoSiBCuNb alloys lies in applications at elevated temperatures, due to the improvement of the soft magnetic response with respect to the conventional FeSi based nanocrystalline alloys.

DOI: 10.1103/PhysRevB.65.024433 PACS number(s): 75.50.Kj, 75.50.Bb, 75.60.−d, 75.30.Gw

INTRODUCTION

The soft magnetic behavior of Fe-rich nanocrystalline alloys, FeSiBCu*M* (Ref. 1) and FeBCu*M* (Ref. 2) with *M* an early transition metal such as Nb, Zr, has been extensively studied during the last ten years.[3] Their excellent soft magnetic response is a direct consequence of their ultrafine grain structure composed of randomly oriented bcc-Fe rich crystals embedded in a residual amorphous matrix,[4] and mainly arises from the averaging out of the magnetocrystalline anisotropy via the magnetic interactions between the two constituent magnetic phases. This magnetic softening is also reinforced by a significant decrease of the magnetoelastic energy due to the reduction of both internal cast-in stresses and the effective magnetostriction.

Within the framework of the random anisotropy model, the magnetic coupling between the ferromagnetic crystals satisfactorily explains the averaging out of the magnetocrystalline anisotropy and thus the excellent soft magnetic behavior.[5] However, the role of the residual amorphous matrix cannot be disregarded (i.e., magnetic decoupling between the crystals above the Curie point of the residual amorphous matrix), and its contribution has been recently analyzed.[6,7] According to these models, the exchange correlation and the structural lengths of the crystalline and amorphous phases constitute the basic parameters.

On the other hand, the demand on bulk soft magnetic materials for high temperature applications has promoted the study of new FeCo based nanocrystalline materials.[8–12] In this new type of nanocrystalline alloys, the higher saturation magnetization and Curie temperature of the crystalline phase determine their magnetic response at high temperatures. However, as reported in Fe-rich nanocrystalline alloys, the effect of the amorphous matrix could play a dominant role in the magnetic coupling between ferromagnetic crystals at high temperature. In this regard, the aim of the present work has been to analyze the effects of the partial substitution of Fe by Co for an FeBSiCuNb base alloy, on the crystallization process and magnetic properties. The results show that the magnetic characteristics of the precipitated crystalline phase play a dominant role in the evolution of the magnetic properties of the thermally treated alloys. While a drastic magnetic hardening is observed in Co-rich samples, soft magnetic behavior is obtained for intermediate Co concentrations close to the equiatomic ($Fe_{50}Co_{50}$) ratio.

EXPERIMENTAL TECHNIQUES

Amorphous ribbons 1 mm wide, about 20 μm thick, and nominal composition $Fe_{73.5-x}Co_xSi_{13.5}B_9Cu_1Nb_3$ ($x=0,5,15,29,36,45,69,73.5$) were obtained by the melt spinning technique. The evolution of the crystallization process was monitored by differential scanning calorimetry (DSC-7) and thermogravimetry analysis (Perkin-Elmer TGA-7), where the temperature dependence of the effective weight of the sample is analyzed under the inhomogeneous field generated by a small permanent magnet. Conventional isochronal thermal treatments (1 h) were performed in an Ar atmosphere at 550 °C. The structure of the samples upon annealing was analyzed by x-ray diffractometry (SIEMENS D-5000) and transmission electron microscopy (JEOL FX 200kV). Axial hysteresis loops at room temperature were measured using a conventional induction method, while the saturation magnetization of the samples were determined by vibrating sample magnetometry (VSM).

RESULTS

Amorphicity of the alloys was checked by x-ray difractometry. Then, the crystallization process from the initial amor-

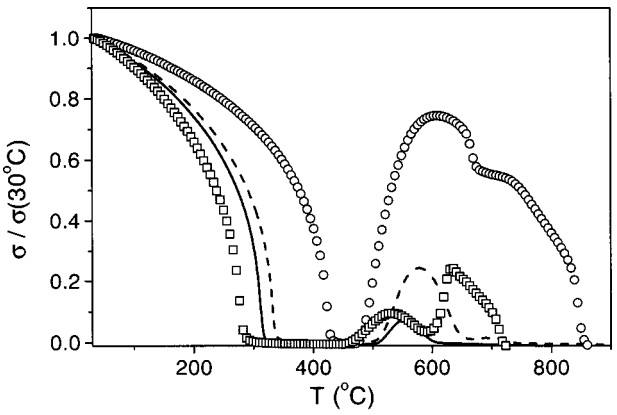

FIG. 1. Thermogravimetry temperature dependence of magnetization σ normalized to its room temperature value [σ (30 °C)], for as-cast alloys $x=$(——) 0, (--) 5, (○) 45, and (□) 73.5.

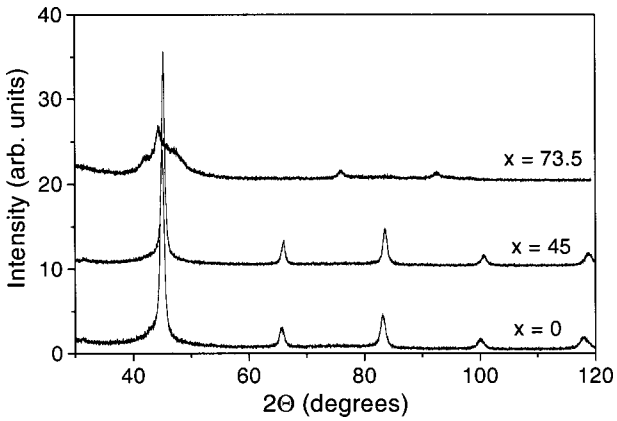

FIG. 2. X-ray diffraction patterns for the $Fe_{73.5-x}Co_xSi_{13.5}B_9Cu_1Nb_3$ heat treated alloys ($T_a=550$ °C, 1 h) for $x=0$, 45, and 73.5.

phous state was followed by thermogravimetry analysis performed at a heating rate of 20 °C/min. Figure 1 shows the magnetization σ under a constant dc field of 100 Oe, versus the measuring temperature T. The initial decrease of $\sigma(T)$, associated to the ferroparamagnetic transition of the initial amorphous phase, is followed by a sharp increase related to the onset of the crystallization process. As Fig. 1 reflects, the beginning of the crystallization process shifts towards lower temperatures with increasing Co content of the alloys x. This decrease is also confirmed through the DSC analysis. Table I summarizes the measured crystallization temperatures as a function of x. For $x\leqslant 45$ two well defined crystallization processes are observed, characterized by crystallization temperatures T_{x1} and T_{x2}, that in the particular case of the Fe-based sample ($x=0$) are correlated to the precipitation of bcc α-FeSi and FeB phases, respectively.[13] For higher Co contents ($x\geqslant 69$), a third crystallization process is also detected reflecting a more complex crystallization process in this range of Co-rich compositions.

The marked temperature gap between T_{x1} and T_{x2} guarantees the precipitation of a single crystalline phase for annealing temperatures T_a below T_{x2}, i.e., $T_a=550$ °C. In order to analyze the structure once the first crystallization process is achieved, the alloys were submitted to isochronal thermal treatments during 1 h at 550 °C. Figure 2 shows the x-ray diffraction patterns after that annealing treatment. As previously reported, the Fe-based sample ($x=0$) is characterized by the precipitation of randomly oriented α-Fe(Si) crystals.[4] As the Co content increases within the range $x\leqslant 45$, the reflexion peaks shift toward higher diffraction angles, reflecting a contraction of the precipitated bcc lattice. In order to estimate the mean error associated with this estimation, the x-ray diffraction patterns were fitted using the Rietveld method.[14] Table II shows the decrease of the mean lattice constant a, as a function of x. For higher Co contents ($x\geqslant 63$), new Co-rich crystalline phases are detected,[15] whose reflection peaks can be mainly associated to fcc and hcp Co phases. The existence of Si in solid solution with Co cannot be completely excluded.

In order to verify the nanocrystalline structure of the samples, transmission electron microscopy (TEM) observations were performed in selected annealed states. Figure 3 shows the characteristic TEM micrograph obtained for $x=45$. As observed, homogeneously distributed nanostructures are obtained, with grain sizes d in the range 8–15 nm. Similar results are obtained by analyzing the broadening of the x-ray peak using the Scherrer formula. The evolution of d versus x is shown in Table III. A maximum value of $d\approx 15$ nm is obtained for intermediate Co compositions ($x\approx 45$).

With respect to the thermogravimetric curves of the previously annealed samples ($T_a=550$ °C, 1 h), $\sigma(T)$ shows the typical evolution of a two magnetic phase system. As an example, Fig. 4 shows $\sigma(T)$ for $x=0$, 5, and 29, normalized to the saturation values obtained by the VSM magnetometer

TABLE I. Crystallization temperatures T_x as a function of the Co content of the samples x obtained through the DSC thermographs.

x (%)	T_{x1} (°C)	T_{x2} (°C)	T_{x3} (°C)
0	553	690	
5	543	687	
29	524	702	
36	512	690	
69	450	644	690
73.5	478	612	645

TABLE II. Dependence of the lattice parameter a for the precipitated α-Fe(Si, Co) crystalline phase [$T_a=550$ °C (1h)] on Co content x.

x (%)	a (Å)
0	2.8403 ± 0.0005
15	2.835 ± 0.005
29	2.8325 ± 0.0004
36	2.8322 ± 0.0004
45	2.8293 ± 0.0004

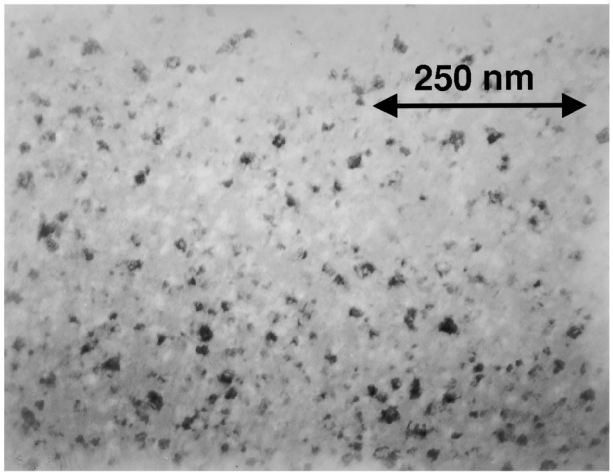

FIG. 3. Transmission electron microscopy (TEM) image for the annealed sample ($T_a = 550\,°C$, 1 h) with $x = 45$.

$[\sigma_s(\text{emu/g})]$. From the analysis of these curves for different Co contents, the evolution of the Curie temperature T_c of the amorphous phase after the segregation of the crystalline phase can be obtained. Figure 5 shows this evolution and its comparison with the T_c value in the precursor amorphous phase (Fig. 1). While for $x \leqslant 36$, T_c does not exhibit significant changes after the crystallization process, it sharply decreases for higher Co contents after nanocrystallization. Moreover T_c for the precipitated crystalline phase can be also estimated through the $\sigma(T)$ curves, assuming the following temperature dependence of the saturation magnetization of the crystalline phase for $T > T_c(\text{amorph})$:[16] $\sigma_s(T) = \sigma_s(0)(1 - T/T_c)^{\beta}$; with $\beta = 0.36$. This critical exponent law is strictly valid close to the Curie point. In fact, the comparison with the T_C values obtained from Fig. 1 give rise to a maximum difference close to 12% for $x = 0$. Such a maximum difference is introduced as an error bar in data displayed in Fig. 5. However, even within this range of estimated error, it can be clearly seen that the main effect of the Co substitution is to increase significantly T_C for $x \leqslant 45$, and subsequently to decrease it for higher Co contents.

Finally, Table III summarizes the coercivity H_c at room temperature after the mentioned thermal treatment as a function of x. As previously reported,[17] H_c drastically increases

TABLE III. Evolution of mean grain sizes d, coercive field H_c, and estimated magnetocrystalline anisotropy k_1 as a function of the Co content of the alloy x.

x (%)	d (nm)	H_c (A/m)	k_1 (J/m^3)
0	11	1.7	14.8×10^3
5	12	3	9.5×10^3
15	13	5	9.5×10^3
29	13	9	9.2×10^3
36	14	7	9.2×10^3
45	15	4	7.8×10^3
69	8	110	
73.5	5	10500	

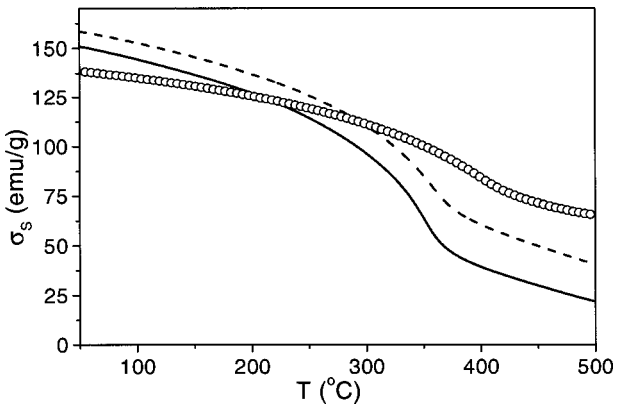

FIG. 4. Thermogravimetric temperature dependence of magnetization σ normalized to the saturation values for the annealed samples ($T_a = 550\,°C$, 1 h): $x = (——)$ 0, (--) 5, and (○) 29.

(up to about four orders of magnitude) with the precipitation of Co-rich phases for $x \geqslant 63$. For $x \leqslant 45$, the main effect of the partial substitution of Co is an initial increase in H_c, followed by a noticeable magnetic softening around $x = 45$.

DISCUSSION

The crystalline α-Fe(Si) phase, characteristic of the Fe based composition ($x = 0$), has been extensively studied.[18] Its ordered form Fe_3Si presents a fcc DO_3-type structure with two nonequivalent Fe sites with a magnetic moment of $1.35\mu_B$ and $2.20\mu_B$ (Fe_{II} and Fe_I, respectively). It has been shown that when transition metal impurities are added to Fe_3Si, in the particular case of addition of Co, a single fcc phase ($Fe_{3-y}Co_ySi$) is observed for $y \leqslant 2.15$, with lattice parameter a, decreasing when Co substitutes Fe into the Fe_{II} sites.[19,20] Thus, in our present case, the detected lattice contraction with x (see Table II) can be correlated to a similar Co substitution and the formation of the ternary FeCoSi phase for $x \leqslant 45$. Taking the lattice contraction in the reported ternary $Fe_{3-y}Co_ySi$ alloys as reference data, the mean composition of the precipitated crystalline phase can be estimated (see Table IV). However, a slight modification must be intro-

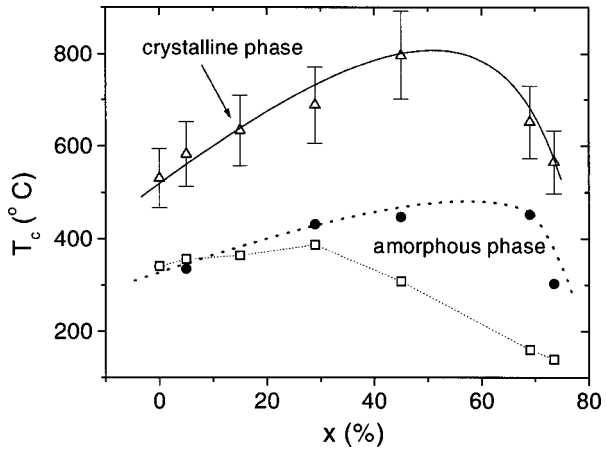

FIG. 5. Curie temperature T_c versus Co content x in the as-cast state (●) and after nanocrystallization: nanocrystalline phase (△) and residual amorphous matrix (□).

TABLE IV. Volume crystalline fraction v_c and estimated composition of the crystalline phase and residual amorphous matrix as a function of the Co content of the alloy x.

x (%)	v_c (%)	Crystalline phase	Residual amorph. phase
0	80	$Fe_{84}Si_{16}$	$Fe_{31}Si_4B_{45}Cu_5Nb_{15}$
5	80	$Fe_{79}Co_5Si_{16}$	$Fe_{26}Co_5Si_4B_{45}Cu_5Nb_{15}$
15	80	$Fe_{67}Co_{17}Si_{16}$	$Fe_{23}Co_8Si_4B_{45}Cu_5Nb_{15}$
29	79	$Fe_{52}Co_{32}Si_{16}$	$Fe_{17}Co_{16}Si_5B_{43}Cu_5Nb_{15}$
36	78	$Fe_{44}Co_{40}Si_{16}$	$Fe_{14}Co_{21}Si_5B_{41}Cu_5Nb_{14}$
45	76	$Fe_{34}Co_{50}Si_{16}$	$Fe_{11}Co_{29}Si_6B_{38}Cu_4Nb_{12}$

duced, since the initial Fe base sample presents a slightly higher a value than the reported stequiometric Fe_3Si phase, that can be ascribed to a higher Fe content ($Fe_{84}Si_{16}$).[21] Similar Fe enrichment for the precipitated crystalline phase has been previously reported.[13,22]

On the other hand, the mean composition of the residual amorphous phase can be also evaluated taking into consideration the volume crystalline fraction v_c estimated through the area under the crystallization peaks obtained by the DSC analysis of the previously annealed samples [i.e., $x=15$: $Fe_{58.5}Co_{15}Si_{13.5}B_9Cu_1Nb_3 = v_c(Fe_{67}Co_{17}Si_{16}) + (1-v_c)(Fe_{23}Co_8Si_4B_{45}Cu_5Nb_{15})$]. The evolution of the composition of both phases indicates that the Co atoms, in addition to partially substituting the Fe in the precipitated crystalline phase, remain in a certain percentage in the residual amorphous matrix. In fact, this rough estimation agrees with the observed evolution of T_c of both magnetic phases with x (see Fig. 5). First, the increase of T_c with x in the crystalline phase ($x \leqslant 45$) can be directly associated with an increase in the Co concentration as observed in $Fe_{3-y}Co_ySi$ (Ref. 19) and $Fe_{1-y}Co_y$ (Ref. 23) crystalline alloys. On the other hand, the decrease of T_c of the residual amorphous matrix with x, supports its enrichment in Co atoms since a similar evolution is observed in FeCo based amorphous alloys.[24,25]

Assuming the phase distribution in Table IV, the saturation magnetization of each magnetic phase can also be estimated. The effective magnetic moment per atom μ_H associated to the precipitated crystalline phase can be evaluated assuming the selective substitution of the Fe_{II} atoms and the following magnetic moment for each constituent: Fe $=1.35\mu_B$ (Fe_{II} sites) and $2.20\mu_B$ (Fe_I sites); Si $=-0.07\mu_B$; Co $=1.70\mu_B$.[19] Table V summarizes μ_H and the saturation magnetization σ_0 for some selected compositions. While μ_H slightly increases with x as a consequence of the higher Co moment with respect to the substituted Fe_{II} atoms, σ_0 in emu/g remains roughly constant due to the higher atomic weight of Co atoms. Moreover, taking the experimental values of the saturation magnetization σ_S(exp), of the annealed alloys measured at room temperature, and assuming $\sigma_0 \approx \sigma_S$(cryst) for the crystalline phase, the saturation magnetization of the residual amorphous matrix σ_S(amorp) is evaluated:

$$\sigma_S(\text{exp}) = v_c\sigma_S(\text{cryst}) + (1-v_c)\sigma_S(\text{amorp}). \qquad (1)$$

Table V summarizes the obtained results where the initial as-cast value σ_S(as-cast) is also included. First, the decrease of σ_S(amorp) with x supports the estimated increase of the Co content of the residual amorphous matrix[23] (see Table IV). In addition to this, the moderate increase of σ_S(amorp) for $x=5$, is in agreement with a similar increase in the initial σ_S(as-cast) of the amorphous alloy (see Table V). Regarding the evolution after nanocrystallization, a slight increase in σ_S(amorp) is observed for $x=5$ with respect to the initial as-cast value correlated with a similar enhancement in T_c (see Fig. 5). On the contrary, the samples with higher Co content, present an opposite behavior, that is, a decrease in σ_S(amorp) and T_C after crystallization with respect to the initial σ_S(as-cast) value. Although the existence of an enhancement in T_C as a result of the exchange polarization of the residual amorphous matrix cannot be completely excluded due to the short distance between grains, the compositional dependence seems to play the dominant role in the observed evolution with x. In fact, if the exchange polarization of the residual amorphous matrix dominates the evolution of T_C, an enhancement with respect to the initial as-cast value should be observed for $29 \leqslant x \leqslant 45$ as the result of the increase of the exchange constant and magnetic moment of the precipitated α-FeCoSi crystalline phase. However, as Fig. 5 shows the Curie point of the residual amorphous matrix presents in this range of compositions an opposite behavior, that is, a decrease with respect to the initial as-cast value.

Thus, according to the previous structural analysis the soft magnetic behavior of the nanocrystalline state for samples

TABLE V. Estimated magnetic moment per atom μ_H and its corresponding saturation magnetization σ_0 of the precipitated crystalline phase, and saturation magnetization, σ_S(amorp), of the residual amorphous matrix. Experimental saturation values of the annealed alloy ($T_a=550\,^\circ$C, 1 h), σ_S(exp), and in the initial as-cast amorphous state σ_S(as-cast).

x (%)	μ_H/μ_B	σ_0 (emu/g)	σ_S(amorp) (emu/g)	σ_S(exp) (emu/g)	σ_S (as-cast) (emu/g)
	(crystalline phase)		(amorphous phase)	(experimental annealed)	(experimental as-cast)
0	1.36	148.0	163.7	151.1	148.9
5	1.37	147.9	198.9	158.1	155.8
29	1.39	147.6	107.6	139.2	127.2
45	1.43	147.5	62.0	127.0	112.42

with $x \leqslant 45$, should be ascribed to the precipitation of an ultrafine FeCoSi phase. On the other hand, the drastic magnetic hardening for Co base compositions ($x \geqslant 69$) would be mainly determined by the precipitation of highly anisotropic Co-rich crystalline phases. This evolution can be analyzed with the help of the random anisotropy model,[26] successfully applied by Herzer[5] to these nanostructural systems. According to this model, the magnetocrystalline anisotropy constant k_1, of the precipitated crystalline phase is averaged out when the exchange correlation length $L_1 = \sqrt{A_1/k_1}$ (A_1 the exchange constant), exceeds the orientation fluctuation length δ of randomly distributed local easy axes ($L_1 > \delta$). On this assumption, H_c is related to the average anisotropy k_{eff} by

$$H_c = p_c \frac{k_{\text{eff}}}{\mu_0 M_s} \approx p_c \frac{k_1^4 d^6}{\mu_0 M_s A_1^3}, \tag{2}$$

where $d = \delta$ and p_c is a dimensionless prefactor.

This model is strictly valid for a single phase crystalline material. However, under certain circumstances the more realistic multiphase nature must be taken into consideration and the role of the residual amorphous matrix cannot be disregarded (i.e., initial stages of nanocrystallization and close to the paramagnetic transition of the residual amorphous matrix). According to modified models,[6,7,27] the magnetocrystalline anisotropy is averaged out when the exchange correlation length of the residual amorphous matrix L_2 is larger than the mean intergranular distance $D = d[1/v_c^{1/3} - 1]$. Then for ($L_2 > D$), k_{eff} can be expressed as

$$k_{\text{eff}} = \frac{v_c^2 k_1^4 d^6}{A^3}. \tag{3}$$

with $A = \sqrt{A_1 A_2}$, A_2: exchange constant of the amorphous phase. However, those cases leading to ($L_2 < D$) would give rise to a magnetic decoupling of the crystals, $k_{\text{eff}} \approx k_1$ and thus to a drastic increase in H_c.

In our present case, due to the high volume fraction, v_c, the crystals are very close to each other, with an estimated mean distance $D \approx 1$ nm. Therefore, the coupling condition with respect to the exchange transmitter capacity of the amorphous phase ($L_2 > D$) is fulfilled even for the highest Co concentrations ($x \geqslant 69$). However, as Table III shows, a drastic magnetic hardening is observed for Co-rich compositions. In these cases, owing to the precipitation of highly anisotropic Co-rich phases, the exchange forces are not able to overcome the magnetocrystalline anisotropy and the condition $L_1 > d$ is not fulfilled. For instance, in the sample with $x = 69$ ($d \approx 8$ nm), taking $A_1 = 10^{-11}$ J/m and $k_1 = 5\ 10^4$ J/m^3 (fcc Co), leads to a reduction in L_1 close to 14 nm, which is comparable with the mean crystalline size. In this case, although the crystals are magnetically decoupled the exchanges forces would slightly smooth the anisotropy value as in the case of nanocrystalline spring magnets.[27]

However, for $x \leqslant 45$ both conditions ($L_2 > D$ and $L_1 > d$) are fulfilled and the magnetic softening results as a consequence of the magnetic coupling between crystals. Considering the experimental H_c and v_c values, $p_c = 0.27$, $A = 10^{-11}$ J/m and $\mu_0 M_s = 1.38$ T (nearly constant for $x \leqslant 45$), the crystalline anisotropy of the precipitated crystalline phase can be estimated through the combination of Eqs. (2) and (3). As summarized in Table III, the partial substitution of Fe by Co results in a decrease in k_1 as it is found in crystalline Fe-Co alloys around 40 % at. Co.[28] Therefore, while the initial slight increase in H_c with x is mainly correlated with the increase in the mean value of d, for $x = 45$ the decrease in k_1 is high enough to overcome the effect of the grain growth giving rise to a noticeable decrease in H_c.

With respect to the influence of the residual amorphous matrix, the decrease of σ_S(amorp) and T_c for $29 \leqslant x \leqslant 45$ should give rise to a diminution of the strength of the magnetic coupling. However, such a magnetic hardening is not observed since the coercivity presents a noticeable magnetic softening around $x = 45$. Although, the suggested decrease in k_1 with x could be hidden by the hardening effect of the residual amorphous matrix, the evolution of the exchange constant of the crystalline phase, A_1, must be also considered. In fact, the increase in this range of compositions of the magnetic moment μ_H, and T_c of the crystalline phase should have associated a parallel increase in A_1. Thus, the opposite contributions of both amorphous and crystalline phases is roughly balanced ($A = \sqrt{A_1 A_2}$) and according to Eq. (3) the effective anisotropy k_{eff} would mainly depend on the magnetocrystalline anisotropy and on the mean grain size of the precipitated crystalline phase.

Finally, we must keep in mind that the technological interest of these new FeCo based nanocrystalline alloys is related to their potential high temperature applications. In this regard, Fig. 4 clearly shows the improvement in the magnetic response at high temperatures (increase of σ_S of the FeCoSi alloys with respect to the Fe base sample). This improvement must be again correlated to the particular properties of the precipitated FeCoSi crystalline phase. In this sense, its higher magnetic moment and Curie temperature optimize the high temperature magnetization response, with respect to the conventional Fe base alloy. New studies are now in progress where the temperature dependence of the magnetization process of this new FeCoSi soft magnetic alloys is analyzed in deep detail.

CONCLUSIONS

The evolution of the structural and magnetic properties with the substitution of Fe by Co for the $Fe_{73.5-x}Co_xSi_{13.5}B_9Cu_1Nb_3$ alloy series is presented in this work. The devitrified state obtained after annealing at 550 °C (1 h) is mainly composed by ferromagnetic crystals (with mean grain sizes in the range of tens of nanometers) surrounded by the residual amorphous matrix. While a α-FeCoSi phase is observed for $x \leqslant 45$, new Co-rich phases are observed for compositions beyond $x = 45$. In spite of the changes in the magnetic characteristics of the residual amorphous matrix with x, the magnetic behavior of the samples are mainly determined by the structural and magnetic properties of the precipitated crystalline phase. In particular, a soft magnetic behavior is obtained for $x \leqslant 45$ ascribed to the magnetic coupling between the α-FeCoSi crystals. The higher Curie temperature of the precipitated crystalline phase

in these ranges of Co concentrations, determines the improvement of their magnetic response at high temperatures with respect to the Fe base alloy.

ACKNOWLEDGMENTS

This work was supported by the Spanish CICYT under Project No. MAT-1999-0422-C02 and the Gobierno de Navarra (Project: Aleaciones ferromagnéticas blandas de interés tecnológico e industrial). The authors wish to thank Professor V. Madurga for experimental support in the themogravimetry measurements and Dr. J. I. Pérez-Landazábal for helpful discussions in the x-ray diffractometry. The TEM study was performed at IFW Dresden (Institut für Metallische Werkstoffe) by Dr. A. Hütten.

*E-mail address: gpolo@unavarra.es

[1] Y. Yoshizawa, S. Oguma, and K. Yamauchi, J. Appl. Phys. **64**, 6044 (1988).
[2] K. Suzuki, A. Makino, N. Kataoka, A. Inoue, and T. Masumoto, Mater. Trans., JIM **32**, 93 (1991).
[3] A. Hernando, J. Phys.: Condens. Matter **11**, 9455 (1999).
[4] G. Herzer, IEEE Trans. Magn. **25**, 3327 (1989).
[5] G. Herzer, Mater. Sci. Eng., A **133**, 1 (1991).
[6] A. Hernando, M. Vázquez, T. Kulik, and C. Prados, Phys. Rev. B **51**, 3581 (1995).
[7] J. Arcas, A. Hernando, J. M. Barandiarán, C. Prados, M. Vázquez, P. Marín, and A. Neuweiler, Phys. Rev. B **58**, 5193 (1998).
[8] M. A. Willard, D. E. Laughlin, M. E. McHenry, D. Thoma, K. Sickafus, J. O. Cross, and V. G. Harris, J. Appl. Phys. **84**, 6773 (1998).
[9] M. A. Willard, M.-Q. Huang, D. E. Laughlin, M. E. McHenry, J. O. Cross, V. G. Harris, and C. Franchetti, J. Appl. Phys. **85**, 4421 (1999).
[10] S. He, K. He, B. Shen, H. Zhang, and H. Guo, J. Appl. Phys. **86**, 6301 (1999).
[11] T. Kemény, D. Kaptás, L. F. Kiss, L. Bujdosó, J. Gubicza, T. Ungár, and I. Vincze, Appl. Phys. Lett. **76**, 2110 (2000).
[12] M. Willard, D. E. Laughlin, and M. E. McHenry, J. Appl. Phys. **87**, 7091 (2000).
[13] F. Zhu, N. Wang, R. Busch, and P. Haasen, Scr. Metall. Mater. **25**, 2011 (1991).
[14] J. I. Perez-Landazabal, M. L. No, G. Madariaga, and J. San Juan, J. Appl. Crystallogr. **30**, 107 (1997).
[15] M. Müller, H. Grahl, N. Mattren, U. Kühn, and B. Schnell, J. Magn. Magn. Mater. **160**, 284 (1996).
[16] A. Slawska-Waniewska, M. Gutowski, H. K. Lachowicz, T. Kulik, and H. Matyja, Phys. Rev. B **46**, 14 594 (1992).
[17] L. Pascual, C. Gómez-Polo, P. Marín, M. Vázquez, and H. A. Davies, J. Magn. Magn. Mater. **203**, 79 (1999).
[18] W. A. Hines, A. H. Menotti, J. I. Budnick, T. J. Burch, T. Litrenta, V. Niculescu, and K. Raj, Phys. Rev. B **13**, 4060 (1976).
[19] V. Niculescu, J. I. Budnick, W. A. Hines, S. Pickart, and S. Skalski, Phys. Rev. B **19**, 452 (1979).
[20] V. A. Niculescu, T. J. Burch, and J. I. Budick, J. Magn. Magn. Mater. **39**, 223 (1983).
[21] R. M. Bozorth, in *Ferromagnetism* (IEEE Press, Trenton, 1993), p. 74.
[22] J. Zbroszczyk, K. Narita, J. Olszewski, W. Ciurzynska, W. Lijun, B. Wysloki, S. Szymua, and M. Hasiak, J. Magn. Magn. Mater. **160**, 281 (1996).
[23] J. G. Booth, in *Ferromagnetic Materials*, edited by E. P. Wohlfarth and K. H. J. Buschow (Elsevier Science Publishers, British Vancouver, 1988), Vol. 4, p. 235.
[24] M. Knobel, R. Sato-Turtelli, and R. Grössinger, J. Magn. Magn. Mater. **116**, 154 (1992).
[25] A. Hernando, I. Navarro, and P. Gorria, Phys. Rev. B **51**, 3281 (1995).
[26] R. Alben, J. J. Becker, and M. C. Chi, J. Appl. Phys. **49**, 1653 (1978).
[27] J. Arcas, A. Hernando, C. Gómez-Polo, F. J. Castaño, M. Vázquez, A. Neuweiler, and H. Kronmuller, J. Phys.: Condens. Matter **12**, 3255 (2000).
[28] R. C. Hall, Trans. Metall. Soc. AIME **218**, 268 (1960).